

Synthesis and characterization of mesoporous alumina for use as a catalyst support in the hydrodechlorination of 1,2-dichloropropane: effect of preparation condition of mesoporous alumina

Pil Kim, Younghun Kim, Heesoo Kim, In Kyu Song, Jongheop Yi*

School of Chemical Engineering, College of Engineering, Seoul National University, Shinlim-dong, Kwanak-ku, Seoul 151 742, South Korea

Received 14 May 2003; accepted 12 April 2004

Available online 15 June 2004

Abstract

Samples of mesoporous γ -aluminas were synthesized by a post-hydrolysis method which contained different mole ratios of stearic acid (surfactant)/Al(sec-OBu)₃ (aluminum precursor). The Ni catalysts supported on aluminas were then prepared by an impregnation method used as catalysts in the hydrodechlorination of 1,2-dichloropropane. The effect of the mole ratio of surfactant/aluminum precursor on the properties of aluminas and supported Ni catalysts was investigated. The dissolution of aluminum occurred during the impregnation step, and the amounts of aluminum dissolved were correlated with the mole ratio of surfactant/aluminum precursor. As the mole ratio of surfactant/aluminum precursor increased, large amounts of aluminum ions were dissolved in the nickel nitrate solution, leading to the formation of large amounts of nickel aluminate species in the supported catalyst. A supported catalyst that contained a large portion of nickel aluminate species was resistant to being reduced to active nickel metal efficient for the hydrodechlorination. When the nickel was impregnated on an alumina, which was prepared with low mole ratio of surfactant/aluminum precursor, the supported catalyst exhibited the enhanced catalytic activity in the hydrodechlorination of 1,2-dichloropropane.

© 2004 Elsevier B.V. All rights reserved.

Keywords: Mesoporous alumina; Surfactant; Aluminum precursor; Hydrodechlorination; Supported Ni catalyst

1. Introduction

Transition aluminas such as γ -Al₂O₃ or η -Al₂O₃ have been widely used in the field of catalysis and adsorption technology [1]. Numerous attempts have been made to synthesize stable and high-quality transition aluminas, because of their potential importance in petroleum industries. Since the discovery of M41S by mobil researchers [2], a number of research groups have also attempted to produce mesoporous aluminas with a high surface area and a narrow pore size distribution [3–8]. In the early stage of the synthesis of mesoporous alumina, difficulty in controlling the hydrolysis rate of aluminum precursors was found to be the crucial problem prior to establishing a systematic strategy for preparing mesoporous silica materials. However, this problem was solved successfully by introducing

a post-hydrolysis method, where small amounts of water were used as a catalyst after micelle formation [3,4]. It has also been reported that pure mesophase aluminas could be synthesized by the reaction of aluminum alkoxides and carboxylic acids in the presence of the controlled amounts of water [5]. After calcination of the synthesized materials, thermally stable and randomly ordered mesoporous aluminas with a high surface area and a narrow pore size distribution were obtained. Another report demonstrated that a mesoporous alumina with a well-ordered pore structure could be synthesized by a nonionic templating method [9].

Nickel catalysts supported on alumina have been utilized in heterogeneous catalytic reactions such as hydrogenation [10], hydrogenolysis [11], and partial oxidation of methane [12]. When a nickel catalyst is supported on alumina by an impregnation method, one of most critical problems encountered in using the resulting nickel/alumina catalyst is the formation of nickel aluminate-like species caused by the

* Corresponding author. Tel.: +82 2 880 7438; fax: +82 2 888 7295.
E-mail address: jyi@snu.ac.kr (J. Yi).

diffusion of Ni^{2+} ions into the alumina lattice. It is known that nickel aluminate species exhibits a poor activity for several hydrogen-involving reactions because of their difficulty in reduction into active metals [13]. It has been reported that the dissolution of aluminum ions during the impregnation step accelerates the formation of nickel aluminate species on the catalyst surface [14].

In a previous study [15] investigating the nickel catalyst supported on a mesoporous γ -alumina by an impregnation method, it was shown that mesoporous γ -alumina could serve as an efficient support for the nickel catalyst for hydrodechlorination reaction. Furthermore, we also found that considerable amounts of surface aluminum species were dissolved during the impregnation step, resulting in the formation of nickel aluminate species. In the preparation of a nickel catalyst supported on mesoporous γ -alumina, therefore, the stability of γ -alumina is an important consideration and needs to be improved. In order to improve the stability of mesoporous γ -alumina as a support for nickel catalyst in the impregnation step, mesoporous γ -aluminas were synthesized under a variety of conditions. The mole ratio of surfactant with respect to the aluminum precursor

was varied for this purpose. The effect of parameters used in preparation of mesoporous γ -alumina on the characteristics and catalytic activities of supported nickel catalysts was investigated extensively. The hydrodechlorination of 1,2-dichloropropane was carried out as a model reaction in this study.

2. Experimental

2.1. Preparation of mesoporous alumina and supported Ni catalyst

Mesoporous γ -aluminas were prepared by a post-hydrolysis method, as described previously [3,4]. All preparation procedures were conducted at room temperature and at atmospheric pressure. In a typical procedure, the required amounts of $\text{Al}(\text{sec-BuO})_3$ (aluminum source) and stearic acid (surfactant) were dissolved separately in sec-butyl alcohol, and the two solutions were then mixed. Water was then added to the mixture at a rate of 1 ml/min, until a white precipitate was formed. The mole ratio of surfactant with

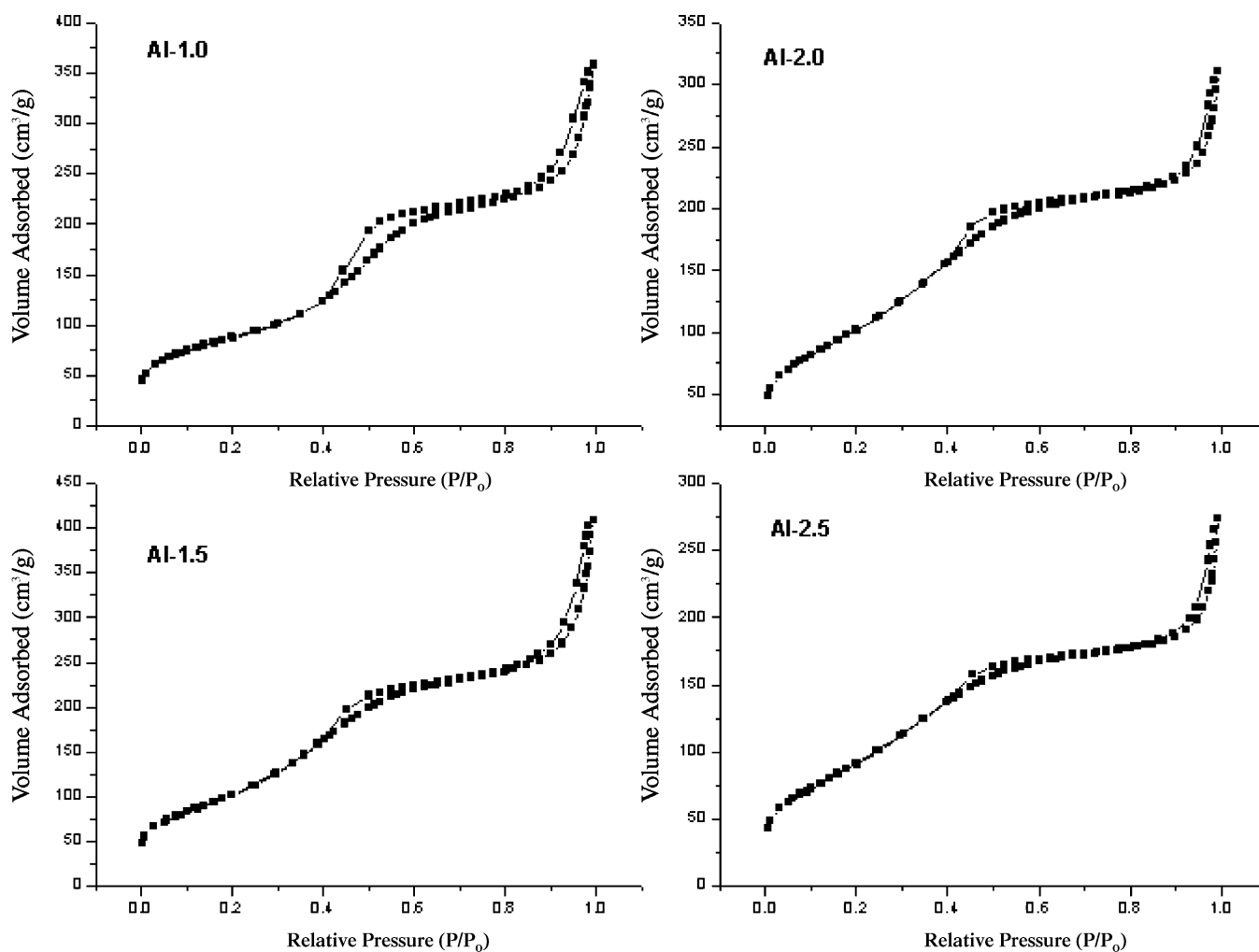


Fig. 1. N_2 adsorption–desorption isotherms of mesoporous aluminas as a function of mole ratio of surfactant/aluminum precursor.

respect to the aluminum precursor was varied within the range of 0.1–0.25, while other preparation conditions were fixed. The resulting slurry was further stirred for 24 h, and subsequently, dried in a stream of air. The crude product was thermally treated at 500 °C for 3 h to yield the final form. The prepared alumina samples were denoted as Al-X, where X represents 10 times the mole ratio of the surfactant/aluminum precursor.

Nickel catalysts supported on alumina were prepared by an impregnation method using nickel nitrate as a nickel source. The prepared catalysts were dried overnight at 120 °C, and then calcined at 500 °C for 5 h in a stream of air. The nickel loading of the supported catalysts was 10 wt.%. The prepared catalysts were denoted as Ni/Al-X.

2.2. Characterization

Small angle X-ray scattering (SAXS) patterns were recorded on a GADDS (Bruker) instrument using Cu K α radiation to analyze the periodicity. Adsorption-desorption isotherms of nitrogen were obtained with an ASAP 2010

(micromeritics) apparatus. Pore size distributions were determined by the BJH method applied to the desorption branch of the N₂ isotherm. The metallic states of the Ni species were confirmed by ultra violet diffuse reflectance spectroscopy (UV-DRS, Perkin-Elmer, Ramda-20 spectrometer) within the range of 200–800 nm. X-ray photoelectron spectra (XPS) were obtained on a AXIS-HS equipment. Temperature-programmed reduction (TPR) measurements were carried out in a conventional flow system with a moisture trap connected to a TCD at temperatures ranging from room temperature to 900 °C (heating rate = 10 °C/min). A mixed stream of H₂ (2 ml/min) and N₂ (20 ml/min) was used as a reducing gas for 0.1 g of catalyst. The amounts of aluminum dissolved [14] in the nickel nitrate solution (10 wt.%) were determined by ICP-AES.

2.3. Hydrodechlorination of 1,2-dichloropropane

The selective hydrodechlorination of 1,2-dichloropropane (DCPA) into propylene was carried out in a continuous flow fixed-bed reactor at atmospheric pressure. Each cata-

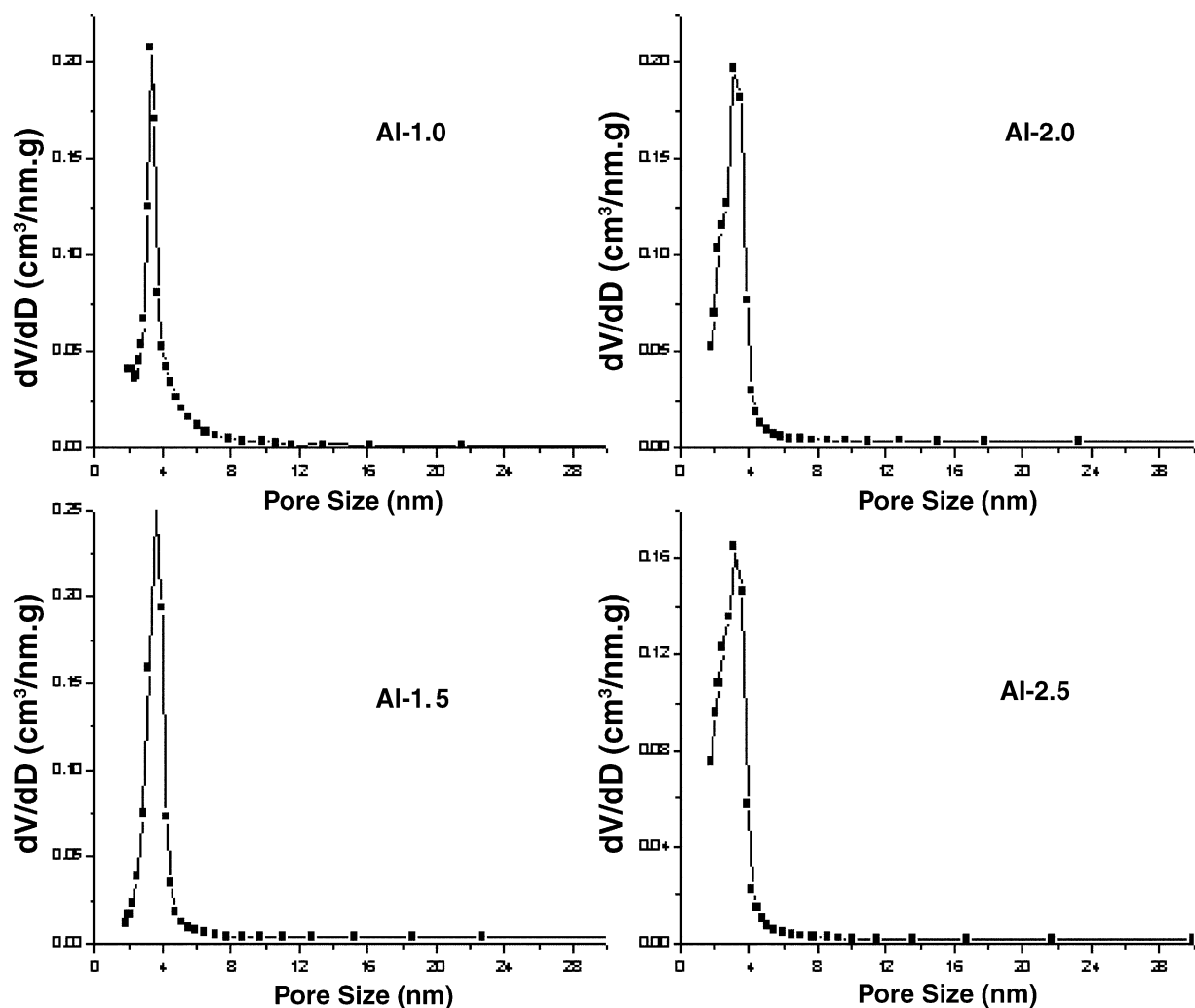


Fig. 2. Pore size distributions of mesoporous aluminas as a function of mole ratio of surfactant/aluminum precursor.

lyst (0.1 g) was charged into a tubular quartz reactor, and activated with a mixed stream of H₂ (20 ml/min) and N₂ (20 ml/min) at 500 °C for 2 h. DCPA (5.13×10^{-3} mol/h) was sufficiently vaporized and fed into the reactor. The catalytic reaction was carried out at 300 °C. The products were periodically sampled and analyzed with a GC–MS and a GC (HP 5890 II, FID). The catalytic reactions were carried out several times for each catalyst under the same conditions. In each run, DCPA conversion and propylene selectivity were within the error range of $\pm 2\%$.

3. Results and discussion

3.1. Physical properties of alumina and the supported Ni catalyst

Fig. 1 shows the N₂ adsorption–desorption isotherms of mesoporous aluminas prepared with a variation of mole ratio of surfactant/aluminum precursor. It is known that N₂

uptake at low partial pressures is due to the monolayer adsorption of probe molecules in the mesopores, and the adsorbed volume up to the relative pressures of ca. 0.4 results from the filling of the mesopores with N₂ [5]. All alumina samples showed IV-type isotherms irrespective of the variation of mole ratio of surfactant/aluminum precursor. The pore size distributions of these alumina samples are shown in Fig. 2. All alumina samples were found to have a relatively narrow pore size distribution centered at around 4 nm.

Fig. 3 and Fig. 4 show the N₂ isotherms and the pore size distributions of the supported Ni catalysts, respectively. Compared to the isotherms of bare alumina supports (Fig. 1), Fig. 3 clearly shows the different shapes for the isotherms. Furthermore, Fig. 4 shows that the supported Ni catalysts exhibited different pore size distributions from those of bare alumina supports (Fig. 2). It is inferred that these results arose from the following two factors; (i) incorporation Ni particles, and (ii) restructuring of catalyst framework caused by aluminum dissolution during the impregnation step. It is likely that the latter is the major factor.

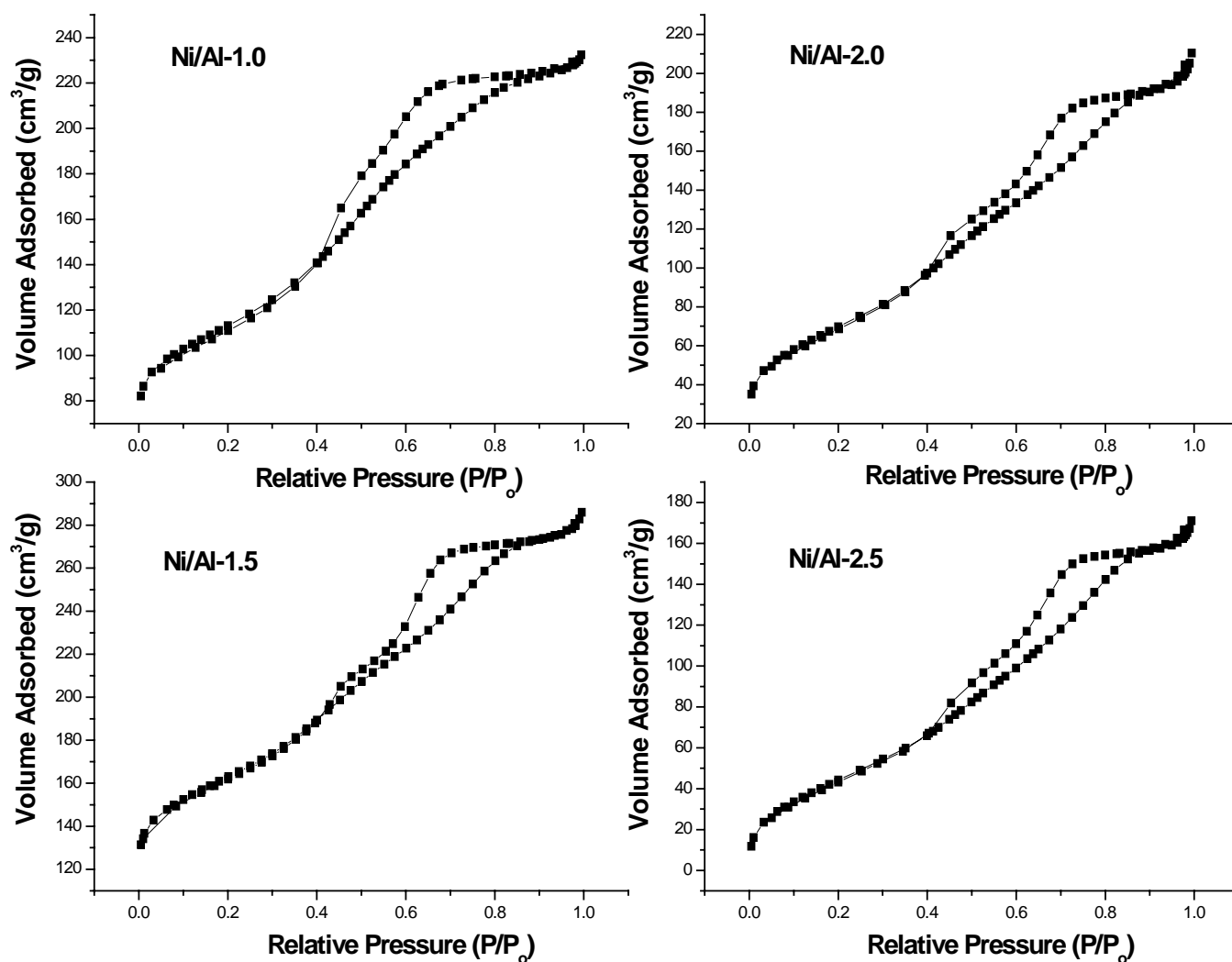


Fig. 3. N₂ adsorption–desorption isotherms of Ni/Al-X catalysts.

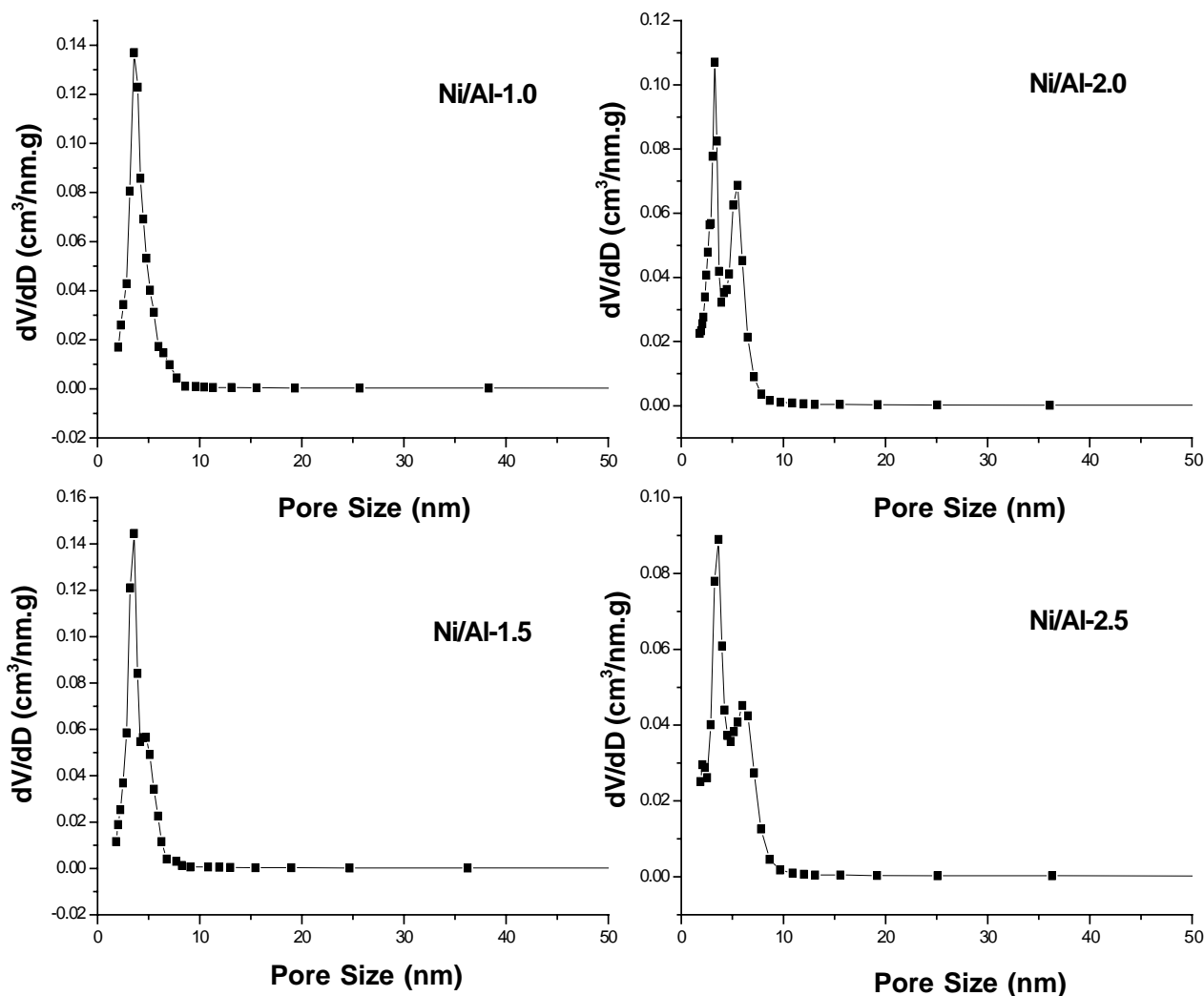


Fig. 4. Pore size distributions of Ni/Al-X catalysts.

The surface area and pore volume of mesoporous alumina and supported Ni catalyst are listed in Table 1. The mesoporous aluminas employed in this work have a relatively high surface area and pore volume as well. The surface area and pore volume of the supported Ni catalyst are lower than those of the corresponding alumina support. Table 2 shows the amounts of aluminum dissolution in a nickel nitrate solution. As listed in Table 2, the amount of aluminum dissolved becomes significant with increasing mole ratio of surfactant/aluminum precursor. Furthermore, Fig. 4 clearly

shows an evolution of a second peak in the pore size distribution with increasing the mole ratio of surfactant/aluminum precursor, as the result of the partial destruction of the pore structure of the alumina. These results are in good agreement with a previous study reporting that significant amounts of aluminum ions are dissolved from the alumina surface during the impregnation of nickel nitrate precursor onto alumina, resulting in the restructuring of the textural properties of the supported nickel catalyst [13]. Therefore, it is reasonable to conclude that the supported Ni catalyst experiencing serious aluminum dissolution during the impregnation step exhibited large deviations of N_2 isotherm and pore size distribution from those of the bare alumina support.

Table 1
Surface area and pore volume of alumina and supported Ni catalyst

	Al-1.0	Al-1.5	Al-2.0	Al-2.5
Surface area (m^2/g)	316	376	380	340
Pore volume (cm^3/g)	0.53	0.60	0.44	0.39
	Ni/Al-1.0	Ni/Al-1.5	Ni/Al-2.0	Ni/Al-2.5
Surface area (m^2/g)	229	230	254	234
Pore volume (cm^3/g)	0.27	0.30	0.30	0.27

Table 2
Amounts of aluminum dissolved in a nickel nitrate solution (10 wt.%)

	Al-1.0	Al-1.5	Al-2.0	Al-2.5
Amounts of aluminum dissolved (ppm)	31	38.9	52.6	64.2

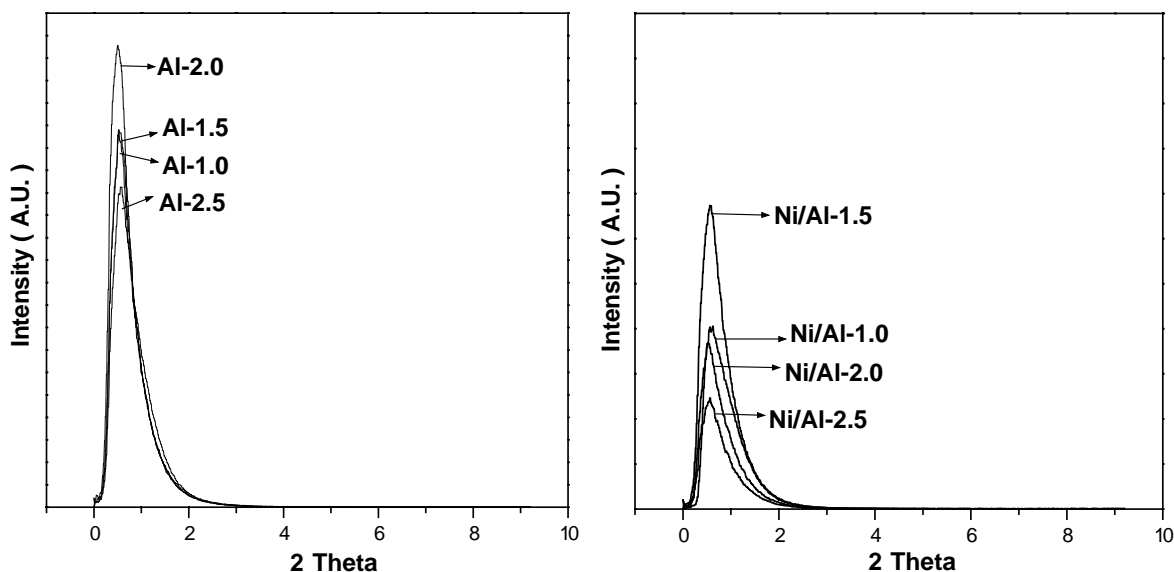


Fig. 5. SAXS patterns of mesoporous aluminas and calcined Ni catalysts.

3.2. SAXS and TEM analyses

The SAXS patterns of mesoporous aluminas and supported Ni catalysts calcined at 500 °C are shown in Fig. 5. It should be noted that SAXS patterns of mesoporous alumina and supported Ni catalyst show a continuous decay with no peaks, indicating a randomly connected pore structure [16]. The SAXS intensity of the supported Ni catalyst was weaker than that of the alumina support. According to the literature [17], the generation of X-ray peaks results from a difference in the scattering power (or scattering contrast) between two building blocks (amorphous wall and channel) of mesoporous materials. Therefore, it is likely that the introduction of Ni particles onto an alumina support would give rise to a weak peak intensity of X-rays.

Fig. 6 shows the TEM images of the calcined mesoporous alumina and the reduced Ni catalyst at 500 °C. The pores

of the alumina support have a wormhole or sponge-like appearance indicative of a highly inter-connected pore system. This result is consistent with the SAXS result. The TEM image of the reduced Ni catalyst showed finely dispersed Ni particles, although some agglomerations larger than the pore size were observed. The sizes of the nickel particles were nearly the same in all catalysts.

3.3. TPR analyses

Fig. 7 shows the TPR profiles of the supported Ni catalysts. The reduction profiles of the supported Ni catalysts could be divided into two zones (T1 and T2), when the reduction profiles were deconvoluted using a Gaussian model. The peak at around 630 °C can be assigned to the typical reduction peak of Ni²⁺ which interacts strongly with γ -Al₂O₃ [14,18]. The second peak at around 780 °C can

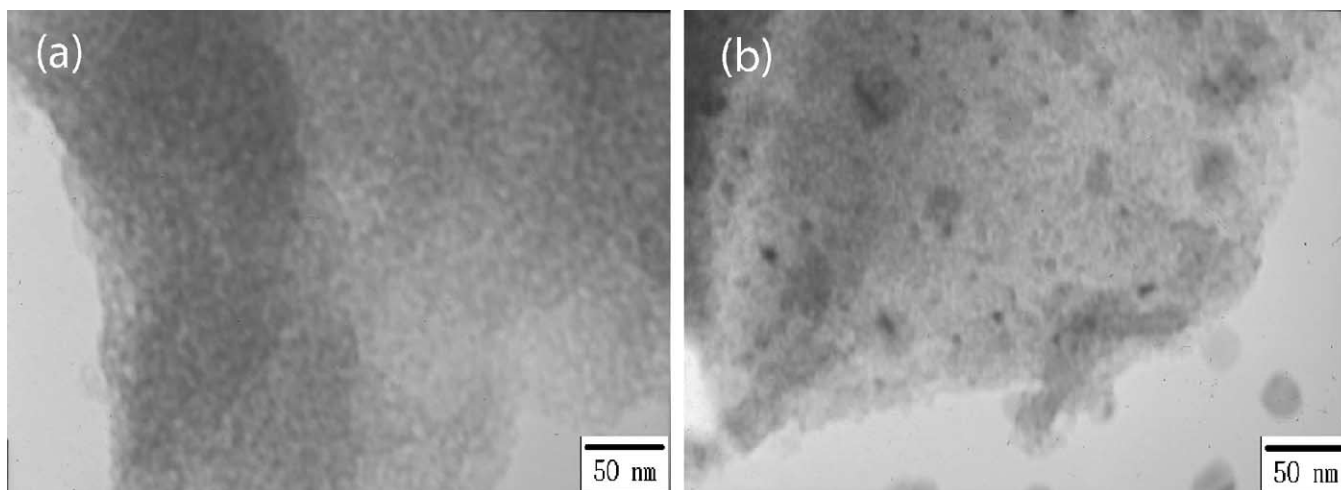


Fig. 6. TEM images of (a) mesoporous alumina (Al-1.5) and (b) Ni catalyst (Ni/Al-1.5) reduced at 500 °C.

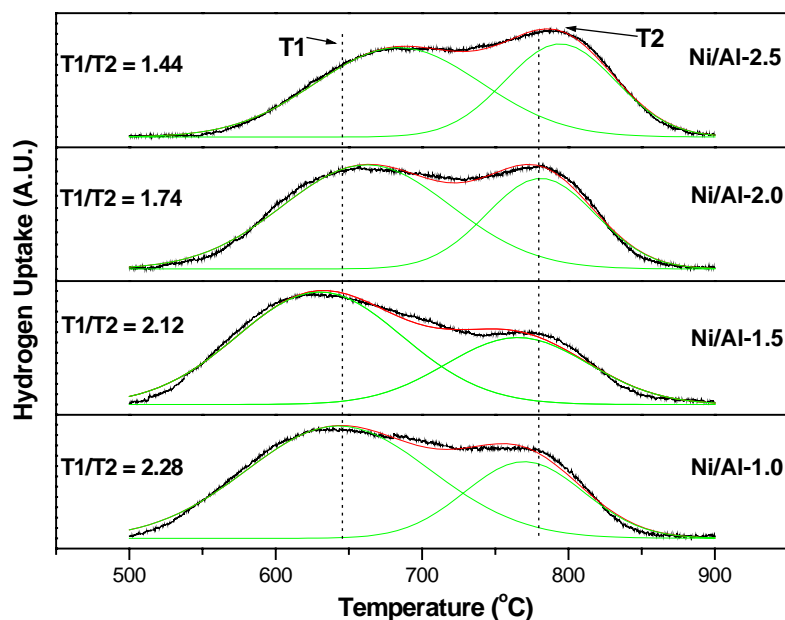


Fig. 7. TPR profiles and peak area ratios of supported Ni catalysts.

be assigned to the reduction peak of nickel aluminate-like species [14,18]. Interestingly, as the mole ratio of surfactant/aluminum precursor increased, the reduction peaks shifted to the higher temperature. It is also noteworthy that the peak areas of Ni^{2+} (T1) relative to the nickel aluminate-like species (T2) decreased with increasing mole ratio of surfactant/aluminum precursor; the portion of nickel aluminate-like species (T2) increased with an increase in the mole ratio of surfactant/aluminum precursor. Upon the impregnation of nickel on alumina from the nickel nitrate

solution, it is known that some parts of Al^{3+} that are located on the surface are dissolved in the solution by hydrogen ions, and the resulting aluminum ions are subsequently readsorbed along with nickel ions [13,14]. This mixed adsorption may yield the formation of some nickel aluminate species on the oxide surface. As listed in Table 2 earlier, the amounts of aluminum dissolution increased with increasing mole ratio of surfactant/aluminum precursor. From these data, we conclude that large amounts of nickel aluminate species are formed when the nickel precursor is impreg-

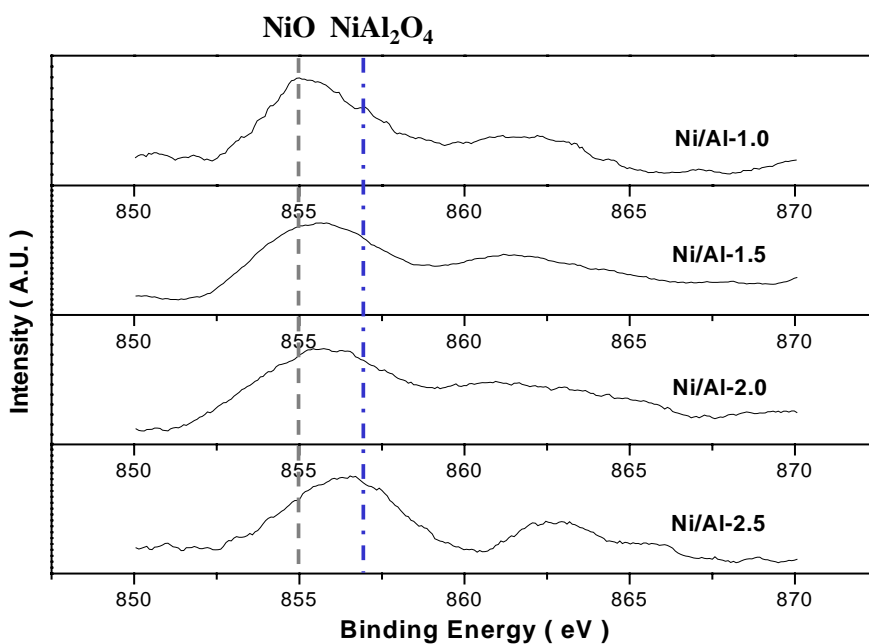


Fig. 8. XPS profiles of supported Ni catalysts.

nated on a mesoporous alumina experiencing large amounts of aluminum dissolution during the impregnation step.

3.4. XPS and UV-DRS analyses

In order to investigate the metallic state of the nickel species, XPS measurements were carried out on the binding energy of the Ni $2p_{3/2}$ level. It is known that the binding energies of Ni in NiO and in nickel aluminate are 855 and 857 eV, respectively [19,20]. As shown in Fig. 8, broad peaks were observed for all the supported catalysts. Importantly, the contribution of binding energy from the nickel aluminate species became strong with increasing mole ratio of surfactant/aluminum precursor. This indicates that Ni catalyst supported on an alumina, which was prepared with a high mole ratio of surfactant/aluminum precursor, retained large amounts of nickel aluminate species in its structure.

In order to confirm the identity of the nickel species and the formation of nickel aluminate, UV-DRS measurements for the supported Ni catalysts were taken. Bands at 715, 377, and/or 410 nm represent the octahedrally coordinated Ni^{2+} species, while the bands in the range of 600–645 nm correspond to the tetrahedrally coordinated Ni^{2+} species [21]. In the nickel aluminate spinel structure, it is well known that the ratio of octahedrally coordinated Ni^{2+} relative to tetrahedrally coordinated Ni^{2+} is dependent on the calcination temperature, the calcination time, and the ramping rate [22]. From this point of view, UV-DRS measurement can be a useful characterization tool for investigating the interaction between nickel and the alumina support. Fig. 9 shows the UV-DRS spectra of the supported Ni catalysts as a function of the molar ratio of surfactant/aluminum precursor. As the molar ratio of surfactant/aluminum precursor increased, the characteristic bands of nickel aluminate appearing in

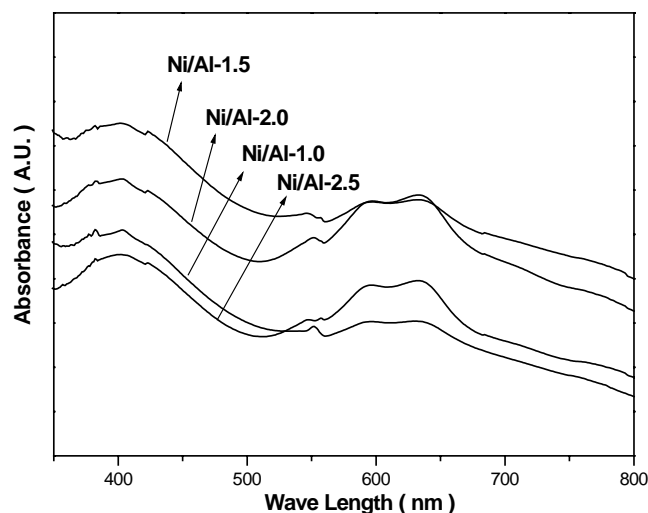


Fig. 9. UV-DRS profiles of supported Ni catalysts after calcination at 500 °C.

the range of 600–645 nm became strong, in good agreement with the TPR (Fig. 7) and XPS results (Fig. 8).

3.5. Hydrodechlorination of 1,2-dichloropropane (DCPA)

Fig. 10 shows the catalytic activities of the supported Ni catalysts in the hydrodechlorination of 1,2-dichloropropane. In the catalytic reaction, propylene and chloropropylene were the major products, while trace amounts of ethylene and chloroethylene were detected by GC–MS. However, no saturated hydrocarbons such as propane or chloropropane were formed. This can be attributed to the activation energy for the hydrogenation of unsaturated hydrocarbons, which is higher than that for the cleavage of C–Cl bonds [23]. Another possible reason for this observation is the rapid

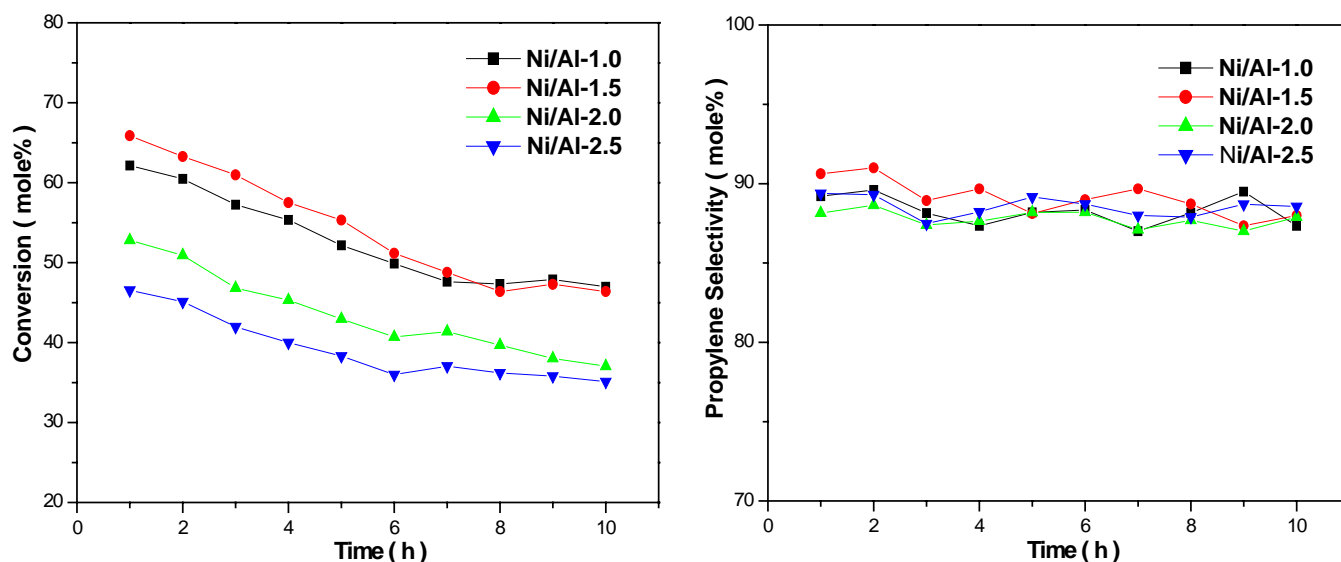


Fig. 10. DCPA conversions and propylene selectivities over supported Ni catalysts at 300 °C with time on stream.

deactivation of available active sites for the hydrogenation, which is caused by the adsorption of HCl on the catalyst surface [24]. It was observed that propylene selectivities over all supported catalysts were nearly the same during the reaction. However, the catalytic activities (DCPA conversion) were roughly decreased with increasing mole ratio of surfactant/aluminum precursor.

We conclude that the different catalytic activities in the model hydrodechlorination reaction resulted from differences in the reducibility of Ni particles. It is well known that the catalytic activity in hydrodechlorination reaction depends on the metal particle size, the interactions between the metal and the support, and the reducibility of the metal oxide [24–28]. In this work, aluminas having almost the same surface area were used as catalyst supports. Therefore, it is likely that the effect of metal particle size on the catalytic activity would be minor compared to the other factors. For the efficient initiation of hydrodechlorination, the chlorinated reactant, along with hydrogen must be adsorbed on metallic nickel (neither nickel oxide nor nickel aluminate). That is, the catalyst having low reducibility shows a poor catalytic activity. Nickel aluminate species could not be easily reduced into active metallic nickel at the conditions used for catalyst pretreatment. Therefore, Ni/Al-2.5 and Ni/Al-2.0 containing large amounts of nickel aluminate species showed suppressed catalytic activities compared to Ni/Al-1.5 and Ni/Al-1.0. A Ni catalyst supported on mesoporous alumina had a low reducibility, when the alumina was prepared with a high mole ratio of surfactant/aluminum precursor.

4. Conclusions

Mesoporous γ -aluminas were synthesized by a post-hydrolysis method with various mole ratios of surfactant/aluminum precursor. The prepared aluminas had high surface areas and narrow pore size distributions centered at ca. 4 nm. It was also found that the aluminas had a randomly connected pore structure, as evidenced by TEM and SAXS measurements. The Ni precursor was supported on the synthesized mesoporous alumina by an impregnation method for use as a catalyst in the hydrodechlorination of 1,2-dichloropropane. The dissolution of aluminum occurred during the impregnation step, and the amounts of aluminum dissolved were related to the mole ratio of surfactant/aluminum precursor. As the mole ratio of surfactant/aluminum precursor increased, larger amounts of aluminum ions were dissolved in the nickel nitrate solution. This resulted in the formation of large amounts of nickel aluminate species in the supported catalyst, a nickel species that could not be easily reduced. In the hydrodechlorination of 1,2-dichloropropane, an enhanced catalytic activity was observed when the Ni precursor was impregnated on an alumina, prepared with a low mole ratio of surfac-

tant/aluminum precursor. In other words, the catalyst showing a high reducibility at the pretreatment conditions had an enhanced catalytic activity. We conclude that a supported catalyst containing a large portion of nickel aluminate in its structure was difficult to be reduced into active nickel metal.

Acknowledgements

This work was supported by National Research Laboratory (NRL) program of the Korea Science and Engineering Foundation (KOSEF).

References

- [1] T.N. Bell, P. Kirszenstejn, B. Czajka, *Catal. Lett.* 30 (1995) 305.
- [2] C.T. Kresge, M.E. Leonowicz, W.J. Roth, J.C. Vartuli, J.S. Beck, *Nature* 359 (1992) 710.
- [3] Y. Kim, B. Lee, J. Yi, *Korean J. Chem. Eng.* 19 (2002) 908.
- [4] Y. Kim, C. Kim, J.W. Choi, P. Kim, J. Yi, *Stud. Surf. Sci. Catal.* 146 (2003) 209.
- [5] F. Vaudry, S. Khodabandeh, M.E. Davis, *Chem. Mater.* 8 (1996) 1451.
- [6] M. Yada, M. Machida, T. Kijima, *Chem. Commun.* (1996) 769.
- [7] S.A. Bagshaw, T.J. Pinnavaia, *Angew. Chem. Int. Ed.* 35 (1996) 1102.
- [8] Y. Liu, W. Zhang, T.J. Pinnavaia, *Angew. Chem. Int. Ed.* 40 (2001) 1255.
- [9] P. Yang, D. Zhao, D.I. Margolese, B.F. Chmelka, G.D. Stucky, *Chem. Mater.* 11 (1999) 2813.
- [10] A.K. Neyestanaki, P. Maki-Arvela, H. Backman, H. Karhu, T. Salmi, J. Vayrynen, D.Yu. Murzin, *J. Mol. Catal. A* 193 (2003) 237.
- [11] S.C. Shekar, J.K. Murthy, P.K. Rao, K.S.R. Rao, E. Kemnitz, *Appl. Catal.* 244 (2003) 39.
- [12] S. Ayabe, H. Omoto, T. Utaka, R. Kikuchi, K. Sasaki, Y. Teraoka, K. Eguchi, *Appl. Catal., A* 241 (2003) 261.
- [13] S.L. Chen, H.L. Zhang, J. Hu, C. Contescu, J.A. Schwarz, *Appl. Catal.* 73 (1991) 289.
- [14] J.A. Mieth, J.A. Schwarz, *Appl. Catal.* 55 (1989) 137.
- [15] P. Kim, Y. Kim, C. Kim, H. Kim, Y. Park, J.H. Lee, I.K. Song, J. Yi, *Catal. Lett.* 89 (2003) 185.
- [16] W. Deng, P. Bodart, M. Pruski, B.H. Shanks, *Microporous Mesoporous Mater.* 52 (2002) 169.
- [17] B. Marler, U. Oberhagemann, S. Vortmann, H. Gies, *Microporous Mater.* 6 (1996) 375.
- [18] R. Molina, G. Poncelet, *J. Catal.* 173 (1998) 257.
- [19] K.M. Lee, W.Y. Lee, *Catal. Lett.* 83 (2002) 65.
- [20] P. Salage, J.L.G. Fierro, F. Medina, J.E. Sueiras, *J. Mol. Catal. A* 106 (1996) 125.
- [21] M.L. Jocomo, M. Schiavello, A. Cimino, *J. Phys. Chem.* 75 (1971) 1034.
- [22] B. Vos, E. Poels, A. Bliet, *J. Catal.* 77 (2001) 198.
- [23] Y.H. Choi, W.Y. Lee, *Catal. Lett.* 67 (2000) 155.
- [24] G. Tavoularis, M.A. Keane, *J. Mol. Catal. A* 142 (1999) 187.
- [25] B. Coq, G. Ferrat, F. Figueras, *J. Catal.* 101 (1986) 434.
- [26] E. Vandesaedt, A. Wiersma, M. Makkee, H. Vanbekkum, J.A. Moulijn, *Appl. Catal. A* 155 (1997) 59.
- [27] S.T. Srinivas, L.J. Lakshmi, N. Lingaiah, P. Prasad, P.K. Rao, *Appl. Catal. A* 135 (1996) 201.
- [28] K. Early, V.I. Kovalchuk, F. Lonyi, S. Deshmukh, J.L. d'Itri, *J. Catal.* 182 (1999) 219.